EUROPEAN SYNCHROTRON RADIATION FACILITY
INSTALLATION EUROPEENNE DE RAYONNEMENT SYNCHROTRON

ESRF

Experiment Report Form

The double page inside this form is to be filled in by all users or groups of users who have had access to beam time for measurements at the ESRF.

Once completed, the report should be submitted electronically to the User Office using the **Electronic Report Submission Application:**

http://193.49.43.2:8080/smis/servlet/UserUtils?start

Reports supporting requests for additional beam time

Reports can now be submitted independently of new proposals – it is necessary simply to indicate the number of the report(s) supporting a new proposal on the proposal form.

The Review Committees reserve the right to reject new proposals from groups who have not reported on the use of beam time allocated previously.

Reports on experiments relating to long term projects

Proposers awarded beam time for a long term project are required to submit an interim report at the end of each year, irrespective of the number of shifts of beam time they have used.

Published papers

All users must give proper credit to ESRF staff members and proper mention to ESRF facilities which were essential for the results described in any ensuing publication. Further, they are obliged to send to the Joint ESRF/ ILL library the complete reference and the abstract of all papers appearing in print, and resulting from the use of the ESRF.

Should you wish to make more general comments on the experiment, please note them on the User Evaluation Form, and send both the Report and the Evaluation Form to the User Office.

Deadlines for submission of Experimental Reports

- 1st March for experiments carried out up until June of the previous year;
- 1st September for experiments carried out up until January of the same year.

Instructions for preparing your Report

- fill in a separate form for each project or series of measurements.
- type your report, in English.
- include the reference number of the proposal to which the report refers.
- make sure that the text, tables and figures fit into the space available.
- if your work is published or is in press, you may prefer to paste in the abstract, and add full reference details. If the abstract is in a language other than English, please include an English translation.

![ESRF] **ESRF**	**Experiment title:** Materials Science Applications of a 3-dimensional x-ray microscope	**Experiment number**: HS-968
Beamline:	**Date of experiment**: from: 1/9 1999 to: 1/9 2000	**Date of report**: 22/2 2000
Shifts:	**Local contact(s)**: U. Lienert, S. Grigull	*Received at ESRF:*

Names and affiliations of applicants (* indicates experimentalists):

H.F. Poulsen[*], L. Margulies[*], S. Schmidt[*], E.M. Lauridsen[*], S.F. Nielsen[*], T. Lorentzen[*], D. Juul Jensen, G. Winther, L.G.Andersen[*], Materials Research Dept., DK-4000 Roskilde.

R.M. Suter, Dept. of Physics, Carnegie Mellon University, Pittsburgh, PA 15213 USA.

U. Lienert, ESRF

Report: We present a number of highlights, all relating to the tracking concept, and all performed at the 3DXRD microscope with microfocused 50-80 keV beams. Other activities, in particular with ceramics, will be summarised in the final report. Work with the conical slit setup [2] and the instrumental upgrading aiming at an improved spatial resolution is ongoing.

Establishment of the tracking technique.
The tracking procedure is a novel x-ray tracing procedure that provides a complete description (position, orientation and elastic strain) of the grains within a specific layer in a powder or polycrystal [5,10]. The method is fast - one layer is characterised within a few minutes - and universally applicable for non-deformed specimens with grains larger than 0.3 microns. In addition the morphology of the grains can be mapped in 3D provided the grains are sufficiently large (> 100 µm). Figs 1 and 2 constitute verifications of the technique.
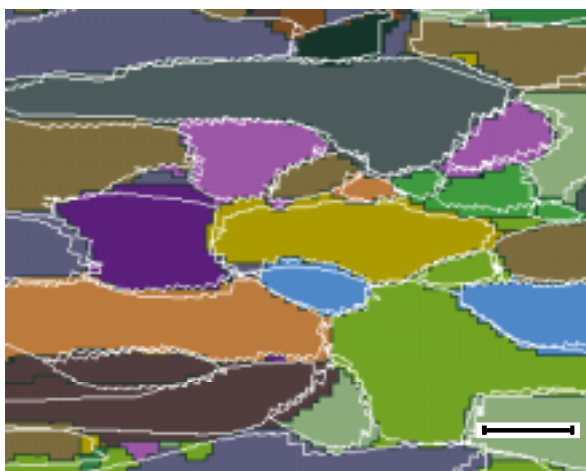

Fig 1.
Map of the grains and grain boundaries on the surface layer of an Al sample. Colours and black lines represent electron microscopy data, white lines results obtained by the 3DXRD technique. The scale bar is 400 µm. The average difference in boundary position between the two techniques is 20 µm. The orientations of grains match within 1 degree. The applied 3DXRD method provides 3D information by mapping layers sequentially, the acquisition time for each layer being a few minutes [15]. An actual application of grain mappings is found in [9].
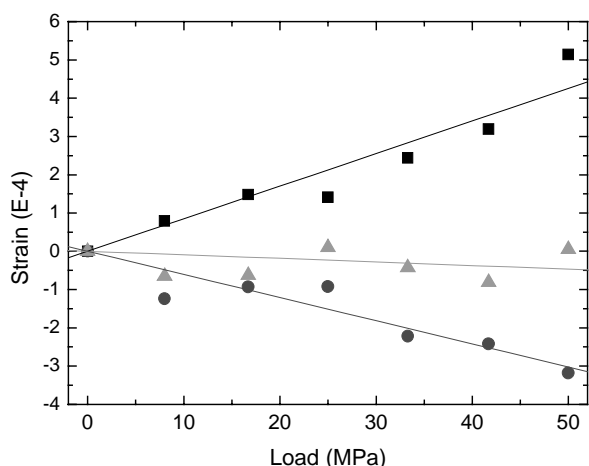
Fig 2.
Evolution of selected elastic strain components for an embedded Cu grain during tensile deformation. The 250 µm sized grain was positioned near the centre of a well annealed specimen with dimensions of 3 x 8 x 50 mm^3. Tracking type data were obtained at 80 keV. Of 21 reflections found, 17 were used in the analysis. The strains ε_{22} (■) and ε_{33}(•) represent directions along the tensile axis and transverse to it, respectively. ε_{23} (▲) is the associated shear component. Lines represent linear fits to the data.The estimated error on the strain is 1×10^{-4}. From [15].

GRAINDEX: indexing of tracking type data

A major task has been the development of a program GRAINDEX that enables automatic indexing of tracking type data (sorting of the spots with respect to which grain they arise from) [14]. GRAINDEX is able to index several hundred grains simultaneously at a speed of a few minutes, sufficient for on-line analysis. The indexing is based primarily on a new crystallographic concept, secondarily on positions and intensities. The software was tested by simulations (100% recovery of 100 randomly oriented grains positioned at the same spot) and by a test experiment on a sintered pellet of Al_2O_3. The number of spots was in this case of order 10000. The program has been used for most experiments reported here [1,5,8,9,10,15,16,17].

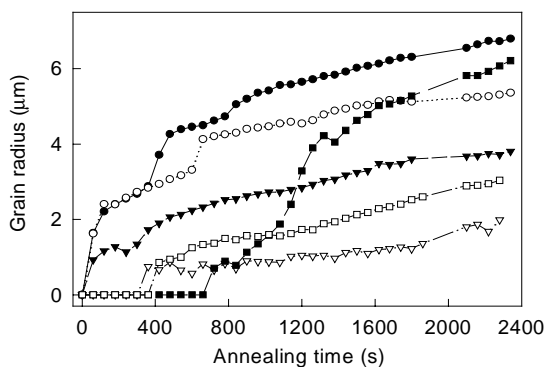## Kinetics of Individual Grains during Recrystallisation.

Fig 3. Growth curves for 6 individual grains during recrystallisation

A number of tracking type studies has been performed with relation to the nucleation and growth of individual internal grains during recrystallisation of Aluminium [3]. The experiments aim at providing statistics of the volume changes of the nuclei as function of orientation (and possibly neighbouring environment). While typically 50 growth curves is obtained during each 3-6 hour annealing, lack of software has delayed the data analysis. Results for the first 6 grains are shown in Fig 3. These relate to 90% cold-rolled 99.5% pure aluminium. The threshold for observation of the nuclei was in this case a radius of 1 micron. In contrast to model assumptions the variations in nucleation time and growth velocity are substantial. Direct evidence is found of an incubation process before the onset of nucleation, and some nuclei are observed to disappear abruptly at an early stage. These results constitute the first data on bulk nucleation processes in metals.

In-situ Measurement of Grain Rotation during Deformation of Polycrystals

We have obtained the first results on the rotation of bulk grains during tensile deformation [1]. The specimen was a 3 mm thick specimen of 99.996% pure Aluminium and an average grain size of 300 μm. Four grains positioned near the centre of the specimen were identified by at least 6 reflections each. The resulting rotations are shown in Fig 4.
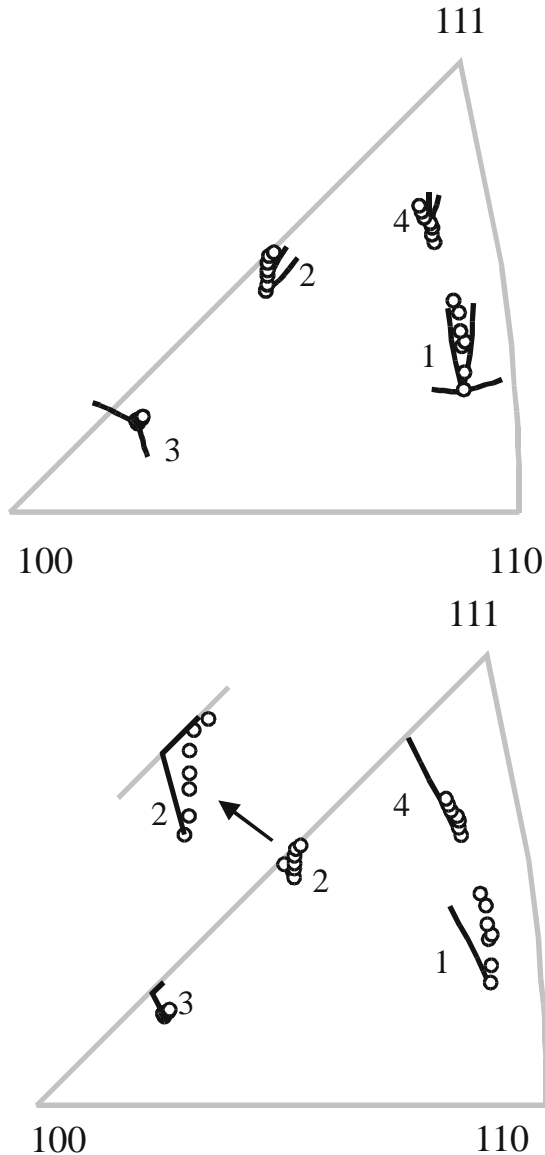

Fig 4.
The dynamics of four embedded Al grains during tensile deformation. Experimental data (**O**) are shown as inverse pole-figures, representing the position of the tensile axis. Strain levels are: 0, 2, 4, 5, 7, 9, and 11%. The instrumental errors are substantially smaller than the symbol size. Comparison is performed with the evolution path from 0% to 11% (——) as predicted by a full constraints Taylor model (upper) and a Sachs model (lower). Several lines associated with the same grain represent degenerate solutions. To allow the comparison, the data set for grain 2 is enlarged.

For the Taylor model, all solutions to the ambiguity problem with a given set of five slip systems are shown, i.e. the model predicts any linear combination of the solutions shown. The rotation rate is seen to be nearly correct, while the experimental direction of the rotation clearly lie to the left of the narrow span of predicted rotation directions for grains 2 and 4. For grain 3, the Taylor model is associated with a large ambiguity, but the experimental rotation towards the <111> corner is totally unpredicted.

The Sachs model has no ambiguity. Here model predictions of the direction agree well with the experimental data for grain 4 but lie to the left of the experimental data for the other three grains. The rotation rates are off by up to a factor of 2.

We conclude that neither model works, but that for three out of the four grains the experimental rotation of the tensile axis lies between the predictions of the Taylor and Sachs models, *i.e.* the grains move towards the predicted dominant stable orientation in the <111> corner. From [1].

Macroscopic pole-figures with a sensitivity of one cell in the dislocation structure.

With two-dimensional focusing and the use of a high-sensitivity camera the 3DXRD microscope can observe (but not map) grains as small as 0.3 µm. Hence, the individual cells in a deformed induced dislocation structure can be characterised, provided they have unique orientations (no spot overlap). Next we may scan the beam over the surface while acquiring a (partial) polefigure at each position. In this way polefigures over mm^3 sized volumes can be provided with a sensitivity of one cell. In comparison it would take tenths of years of electron microscopy work (EBSP) to map similar volumes, and in the end the sample would be reduced to a pile of dust.

These properties make 3DXRD very interesting for nucleation studies. In particular, one may learn what the structure of the deformed material was at the nucleation site prior to nucleation. A first experiment of this kind has been performed [17]. An Al single crystal was cut with the S orientation {123}<634>. The crystal was channel die deformed to a strain of $\varepsilon = 1.5$. An overnight EBSP scan of the deformed structure resulted in 5×10^3 orientations which all were confined around the main poles, cf Fig 5a. Next in the partially recrystallised piece, within an interior volume of $V_0 = 2 \times 10^8 \ \mu m^3$ 5 nuclei were found with orientations within an area A, also marked in Fig 5a. The positions seemingly suggest that nuclei can emerge with orientations not present in the deformed material. That would be contradictory to the present understanding of the nucleation process.

3DXRD measurements on an as-deformed specimen revealed distinct spots with an angular spread given by the set-up (1 deg). These were identified as cells. Those appearing with orientations farthest away from the poles are plotted in Fig 5b. Approximately 15 of these spots are confined with the area A, corresponding to an area fraction of $\approx 2 \times 10^{-7}$. In conclusion, for this particular specimen the tails of the poles is found to spread out over the whole polefigure. Such results could not have been obtained by other means. Furthermore the potential for *in-situ* nucleation and recovery studies is evident.
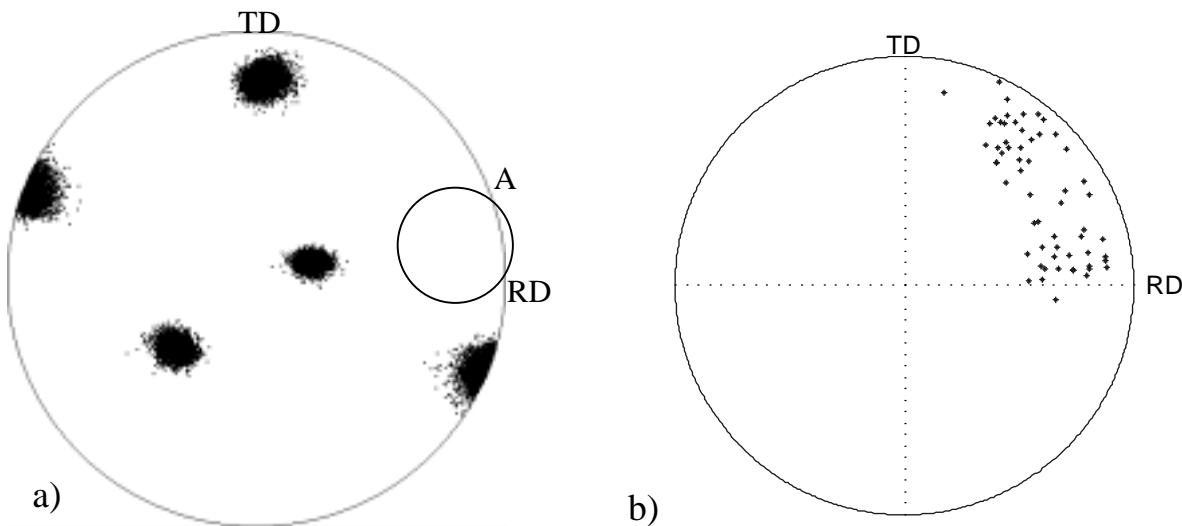

Fig 5. (111) polefigures generated of a deformed single crystal generated by (a) EBSP data from a 1x3 mm^2 grid on the surface, and (b) 3DXRD results on an interior volume of size 1x1x0.01 mm^3. From [17].

Risø 3DXRD Publications 2000-2001
1. L. Margulies, G. Winther and H.F. Poulsen. To appear in Science.
2. S.F. Nielsen, A. Wolf, H.F. Poulsen, M. Ohler, U. Lienert, and R.A. Owen. J. Synchrotron Rad., **7**, p. 103-109 (2000).
3. E.M. Lauridsen, D. Juul Jensen, H.F. Poulsen and U. Lienert. Scripta matter, **43**, p. 561-566 (2000).
4. U. Leinert, H.F. Poulsen, R.V. Martins and Å. Kvick. Materials Science Forum, **347-349**, p 95-100 (2000).
5. D. Juul Jensen, Å. Kvick, E.M. Lauridsen, U. Lienert, L. Margulies, S.F. Nielsen and H.F. Poulsen. Mat. Res. Soc. Symp. Proc., **590,** p. 227-240 (2000).
6. U. Lienert, R. Martins, S. Grigull, M. Pinkerton, H.F. Poulsen and Å. Kvick. Mat. Res. Soc. Symp. Proc, **590**, p. 241-246 (2000).
7. R.V. Martins, S. Grigull, U. Lienert, and H.F. Poulsen. Proc. of 20th Risø Int. Symp. on Mat. Science, 6-10 Sept 1999, p. 411-416.

8. S.F. Nielsen, E.M. Lauridsen, D. Juul Jensen, H.F. Poulsen. Proc. ICSMA-12. In press.
9. S.F. Nielsen, W. Ludwig, D. Bellet, E.M. Lauridsen, H.F. Poulsen and D. Juul Jensen. Proc. of 21st Risø Int. Symp. on Mat. Science, Risø 4-8 September 2000, p. 473-478.
10. D. Juul Jensen and H.F. Poulsen. Proc. of 21st Risø Int. Symp. on Mat. Science, Risø 4-8 September 2000, p. 103-124.
11. D. Juul Jensen. Chap 8 in Electron Backscatter Diffraction in Materials Science. Eds. A.J. Schwartz el al. Plenum Publishers, New York, p. 91-104 (2000).
12. R.V. Martins, U. Lienert, L. Margulies, A. Pyzalla, to appear in J. Neutron Research.
13. R.V. Martins, S. Grigull, U. Lienert, L. Margulies, A. Pyzalla. Proc. ICRS-6, Oxford, United Kingdom, 1, 90 (2000)

Selected pre-prints:
14. E.M. Lauridsen, S. Schmidt, R.M. Suter and H.F. Poulsen. Submitted for J. Appl. Cryst.
15. H.F. Poulsen, S.F. Nielsen, E.M. Lauridsen, R.M. Suter, L. Margulies, T. Lorentzen, D. Juul Jensen Pre-print.
16. T. Lorentzen, L. Margulies, H.F. Poulsen. Pre-print
17. H.F. Poulsen. Pre-print